Supplement for: Mercury mobility, colloid formation and methylation in a polluted fluvisol as affected by manure application and flooding-draining cycle.

Lorenz Gfeller[1], Andrea Weber[1], Isabelle Worms[2], Vera I. Slaveykova[2], Adrien Mestrot[1]

1Institute of Geography, University of Bern, Hallerstrasse 12, 3012 Bern, Switzerland
2Environmental Biogeochemistry and Ecotoxicology, Department F.-A. Forel for environmental and aquatic sciences, School of Earth and Environmental Sciences, Faculty of Sciences, University of Geneva, Uni Carl Vogt, Bvd Carl-Vogt 66, CH-1211 Geneva 4, Switzerland
Correspondence to: Adrien Mestrot (adrien.mestrot@giub.unibe.ch)

(22 Pages, 6 Tables, 14 Figures)

Table of contents

List of Figures

List of Tables

S1 Sampling site and soil sampling

Soils were sampled from agriculturally used fields situated between Visp and Raron in the Rhone Valley Wallis, Switzerland. The sampling location is situated next to a wastewater discharge channel 5 km downstream of a chemical plant (acetaldehyde production) into which the company released their untreated effluents form the 1930's to the 1970's. There, the fields were subject to Hg pollution by Hg contaminated canal sediments (Grossgrundkanal) which were used for fertilization of the nearby fields until the 1980s, when a new water treatment plant was installed. Ever since the polluted soils has been ploughed and turned over. Pollution decreases gradually with distance from the canal and the soil marks a sharp decrease at the plowing horizon at ca. 30 cm depth (Gygax et al., 2019; Glenz and Escher, 2011). Further, an artificial dam separates the channel from the fields inhibiting fast drainage of the fields after heavy rain events.

Samples were taken on 30th of September 2019 along a Hg gradient on a cornfield and a pasture field. Exact coordinates are given in Table S1 a map of the area is shown in Fig. S1. A composite sample of approximately 10 kg of soil was sampled from 10 points along the Hg gradient. After sampling, roots were removed and the samples were pulled in a HDPE bucket, well homogenized, filled in PE zip bags and stored on ice for transportation. In the laboratory, one part of the fresh soil was sieved to <2 mm, further homogenized and used for the incubation. The other part was stored at -20° C.

Fresh liquid manure was sampled from a slurry pit of a cattle farm close to the sampling site. This manure is frequently used to fertilize the soils in the area. Two liters of sample were taken after homogenizing the manure in the slurry pit with an agitator for more than 10 minutes. The samples were kept on ice in HDPE bottles for transportation. In the laboratory, the manure was sieved to <0.5 mm and homogenized. The sample was divided in 2 aliquots and kept for storage at -20° C for characterization and 4° C for addition to the incubation.

S2 Laboratory Materials

Trace metal grade acids, HPLC grade solvents, and ultra-pure water (>18.2 MΩ·cm at 25 °C, Milli-Q® IQ 7000, Merk, Darmstadt, Germany) were used in this study. Glassware was cleaned by soaking in acid baths (both 10% HNO3 and 10% HCl) for at least 24 h and rinsing three times with ultra-pure water. Further, jars used for the incubation were sterilized in an autoclave for a minimum of 30 min at 120°C. Soil solution samples were stored in Corning® sterile PP tubes for trace metal, DOC and ion chromatography (IC) analyses. Borosilicate glass vials with PTFE caps (Wheaton®, DWK Life Sciences GmbH, Wertheim/Main, Germany) were used for storage of Hg soil solution samples.

S3 Chemical characterization of soil and soil solution

All solid samples were freeze dried to avoid a loss of Hg prior to analyses (Hojdová et al., 2015). After drying, the samples were milled and homogenized using an automatic ball mill (MM400, Retsch, Haan, Germany) with stainless steel beakers and balls. In between samples, the beakers were cleaned using phosphate free detergent (RBS™), deionized water and ethanol.

Pre-incubation was conducted in 10 L HDPE buckets in the dark for 7 days at 22 °C and 60% relative humidity (RH) in order to prevent high microbial respiration at the onset the experiment. Microbial respiration is likely to be increased by sieving the soil. After pre-incubation, 50 g of each soil were sampled and oven dried in order to determine moisture content or soil dry weight.

Soil Hg concentrations were measured by thermal desorption atomic fluorescence spectroscopy (DMA-80 evo, Milestone Srl, Sorisole) with a limit of detection of <0.01 ng Hg. Soils were analyzed in a working range of 300 - 800 ng Hg. Blank background levels after a 500 ng Hg standard were <1 ng Hg. After every 10^{th} sample, two liquid standards (300 ng and 500 ng Hg from a 1 mg L^{-1} Hg standard solution (ICP inorganic Hg standard solution, TraceCERT®, Sigma-Aldrich, St. Louis, United States of America) were measured to check the instruments stability and to calculate correction factors. Recovery of liquid standards was within the range of 95 to 105 %.

Soil metals were leached by microwave assisted acid digestion (250 mg soil, 4ml 69 %, HNO_3, 2 ml H_2O_2). The leachate and soil solution trace and major metal concentrations (in 1% HNO_3) as well as soil solution HgT (in 1% HNO3, 0.5% HCl) concentrations were quantified by Inductively Coupled Plasma Mass Spectrometry (ICP-MS; 7700x ICP-MS, Agilent Technologies, Santa Clara, United States of America). Calibration curves were prepared fresh from both a multi element and a Hg standard solution (TraceCERT®, Sigma-Aldrich, St. Louis, United States of America). An internal standard of Indium (m/z 115) or Thallium (m/z 205) was continuously injected for trace metals and Hg, respectively. Calibration standards were measured repeatedly, during the run to check the stability of the system. The rinsing protocol shown in Table S2 was used during HgT analyses in order to avoid memory effects. The LOD for Hg in soil solution was <0.01µg L^{-1} for all soil solution analyses.

A selective HCl-DCM extraction described elsewhere was optimized for high throughput (64 Samples per run) to extract soil methylmercury (MeHg) (Brombach et al., 2015; Gygax et al., 2019). Briefly, 250 mg of sample was suspended in 5 mL of 35% HCl and 5 mL ultrapure water in a 20 mL borosilicate glass vial (Wheaton, Milleville, NJ, UK). After 30 min overhead shaking, the vial was centrifuged for 15 min at 680 g (3500 rpm) and the supernatant transferred a second 20ml vial. Then, the lipophilic organic Hg was extracted by addition of 5mL DCM and overhead shaking for 60 min. The DCM solution was pipetted of in a third 20 mL borosilicate glass vial. For aqueous back extraction 2 mL of 0.1% L-Cysteine were added to the DCM extract and the DCM was evaporated with a constant flow of N_2 on a heating bloc at 50°C. The samples where weighted using an analytical balance after each extraction step to correct for sample losses upon pipetting or evaporation. Detailed validation of this method can be found in Gygax et al., 2019. The final extracts were stored at 4°C and analyzed within 48 hours. They were analyzed by coupling a High-Pressure Liquid Chromatograph (HPLC 1200 Series, Agilent Technologies, Santa Clara, United States of America) to the ICP-MS (HPLC-ICP-MS). The mobile phase consisted of 0.1% L-Cysteine (98%) and Methanol (2%). The detailed HPLC method is given in Table S3. Table S4 contains certified reference

material (CRM) concentrations and recoveries of Hg and MeHg. Limit of detection (LOD) was calculated from the daily calibration curves. The LOD was <0.02 µg L^{-1} for the HPLC-ICP-MS method and <0.16 µg kg^{-1} in soil samples.

Soil Carbon (C), Nitrogen (N) and Sulfur (S) were measured with an Elementar® vario EL analyzer. After every 15^{th} sample, standards of sulfanilic acid and glutamic acid were measured to assure the instruments stability and to calculate correction factors. SOM was determined by loss on ignition (LOI) (550°C for 2h). Organic Carbon (OC) was calculated by subtracting the C concentration of the LOI sample from the original C concentration.

Soil pH was measured in an equilibrated 0.01M $CaCl_2$ solution (1:5 soil:liquid ratio) using a pH-probe (SenTix® 41, WTW, Weilheim, Germany). The probe was calibrated using a two-point calibration using standard solutions (ROTI® Calipure, ROTH, Arlesheim, Switzerland) of pH 7 and 9. During the incubation, pH probes for soil solution pH were calibrated on each sampling day. Oxidation reduction potential (ORP) was measured using a ($Hg/HgCl_2$) ORP probe (Lazar Research Laboratories, Los Angeles, United States of America) and checked with a 200mV ORP standard solution (Hach Company, Loveland, United States of America) on each sampling day.

Soil solution major inorganic ions were analyzed by Ion Chromatography using a Dionex Aquion™ conductivity detector system (Thermo Fisher Scientific Inc., Waltham, United States of America). Details on instrument specifics are given in Table S5.

X-ray diffraction analyses (XRD) was performed on both soils (HMLC and LMHC). XRD powder patterns were measured with a Panalytical $CubiX^3$ diffractometer using a Cu tube (Kα-radiation: λ=1.54Å at 45kV/40 mA), secondary monochromator and automatic divergence slits. 2 theta diffractograms were processed using PANalytical X'Pert HighScore Plus.

Colloidal size fractions and elemental concentrations of the filtrates were analyzed by Asymmetrical Flow Field-Flow Fractionation (AF4, AF2000, Postnova analytic, Landsberg am Lech, Germany) coupled to a UV_{254nm} absorbance detector, a Fluorescence detector (RF-20A, Shimazu, Reinach, Switzerland) and an ICP-MS (7700x, Agilent Technologies, Santa Clara, United States of America). The hydrodynamic size and small colloids molecular mass were calibrated externally. The relationship between molecular mass and hydrodynamic diameter is also given in Fig. S5e. Hydrodynamic diameter calibration was obtained using Hc3 (d_h = 7 nm) and ultra-uniform gold nanoparticles (d_h = 19 ; 39 ; 59 nm). The bigger nanoparticles elute after the end of fractionation when the crossflow is turned off (xf0, red vertical lines at retention time of 20.8 min), while using a linear decrease in crossflow starting at 2 mL min^{-1} over 20 minutes (xf2grad). In this case, the upper size limit of fractionation was evaluated at d_h = 45 nm (Fig. S5a). In the case of a linear decrease of crossflow starting at 1 mL min^{-1} (xf1grad, B), this upper limit rose to d_h =80 nm, and most of the colloidal Hg is eluted before the end of elution. As shown in Fig. S5c, the size of small Hg-particles (indicated with a *) is identical while using one or the other program. Based on the effective cut-off of the filter use for preservation (450nm), the upper size of colloids was surprisingly low, but suggest artefactual removal of higher size colloids. The recovery of those was shown to be more effective using selective centrifugation and filtration with 5 µm cut-off and the use of lower ionic strength mobile phase (µM) than the one used (mM) may probably have increased the interaction of larger inorganic colloids, if present, with the AF4 membrane. For the sample (HMLC +MNR, day 2) shown in Fig S5, it must be noted however that the Hg recovery was of 70% and

74% for xf2grad and xf1grad respectively, suggesting that the loss of bigger colloids has little influence on Hg behavior. For the xf2grad program, the elution of smaller colloidal Hg was related to molecular mass (Mw) using separate injections of PSS (Fig. S5d) and related to hydrodynamic size elution (Fig. S5e).

To further characterize the colloids, we collected fractions of soil solution during AF4 runs by using a T-piece. Factory new, borosilicate headspace GC-vials were used for fraction collection. During the manual fraction collection vials were constantly flushed with argon. After fraction collection the samples were kept stable in 0.01M NH_4NO_3 in air-tight GC vials at 4°C in the dark until further analyses (> 240 days). The collected fraction were studied by Continuous Flow Analysis Inductively Coupled Plasma Time-Of-Flight Mass Spectrometry (ICP-TOF-MS). The ICP-TOF-MS used in this study is the commercially available icpTOF (TOFWERK AG, Thun, Switzerland). The instrument uses the ICP generation, ion-optics, and the collision/reaction cell (Q-Cell) of an iCAP-RQ instrument (Thermo Scientific, Bremen, Germany). In the icpTOF, the original quadrupole mass analyzer of the iCAP-RQ is replaced by a quadrupole notch filter and TOF mass analyzer, both built and integrated by TOFWERK. Further information about the instrumentation can be found elsewhere (Erhardt et al., 2019). Rh in 1% HNO_3 was introduced as an internal standard using a T-piece directly before the nebulizer.

S4 Incubation and sampling setup

Scheme of the incubation setup is shown in Fig. S2. During the incubation, the MCs were covered with parafilm which could not fully prevent exchange with the ambient air. The flooding and draining scheme are given in Fig. S3. A list as well as a flow chart of sample preparations and aliquots for the specific analyses is given in Table S6 and Fig S4.

S5 Complementary statements about colloidal fraction and nanoparticulate formation.

We visually observed black precipitates (Fig. S8 in MCs (HMLC +MNR)) suggesting the precipitation of sulfide minerals and potentially HgS(s). However, we did not observe any sulfur nor Hg signals during the continuous flow ICP–TOF–MS run. This is presumably due to the long storage time and unideal conditions during sample preservation until analyses (> 240 days).

Tables

Table S1: GPS coordinates of the sampling locations.

Sample	Latitude	Longitude
Corn field (HMLC)	46°17′59.900″N	7°49′43.124″E
Pasture field (LMHC)	46°18′04.825″N	7°49′00.229″E
Slurry pit manure (MNR)	46°18′10.435″N	7°49′56.082″E

Table S2: Rinsing protocol for HgT analyses by ICP–MS

Solution	Contents	Rinsing time
Matrix for all samples	1 % HNO3 + 0.5 % HCl	-
Washing solution 1	Ultrapure water	5 s
Washing solution 2	0.6% v/v NH_4OH 0.8% v/v H_2O_2 0.01% v/v Triton X100 0.1% w/v EDTA Diluted 1:10 before use.	40 s
Washing solution 3	5 % HNO3 + 5 % HCl %	30 s
Washing solution 4	1 % HNO3 + 0.5 % HCl	40 s

Table S3: HPLC method details for MeHg analyses

Parameter	HPLC-ICP-MS
HPLC Column	Zorbax SB-C18 4.6 x 150 mm, 5 µm
Injection volume	100 µL
Column temperature	20°C
Mobile phase flow rate	1 ml min^{-1}
Flow rate	
Mobile phase composition	2 % MeOH 98 % of 0.1 % w/v L-cysteine & 0.1 % L-cysteine·HCl·H_2O pH = 2.3

Table S4: Measured CRM concentrations and recoveries for MeHg and Hg. MeHg was measured by HCl-DCM extraction HPLC–ICP–MS. Hg was analyzed by thermal desorption AFS using a DMA-80 evo.

CRM	Type	MeHg (µg kg^{-1})	$MeHg_{recovery}$ (%)	n	Hg (µg kg^{-1})	$Hg_{recovery}$ (%)	n
ERM® - CC580	Estuarine sediment	77.3 ± 3.3	103.1	3	-	-	-
SRM® 2709a	Agricultural soil	-	-	-	906 ± 57	100.7	9
NRC® PACS-3	Marine sediment	-	-	-	3155 ± 149	105.8	3

Table S5: Ion Chromatography method.

Analytes	Pre column	Column	Suppressor	Eluent	Flow rate
Cations	Dionex™ IonPac™ CG12A 4x50 mm	Dionex™ IonPac™ CS12A 4x250 mm	Dionex™ CSRS™ 300	20mM Methanesulfonic Acid (MSA)	1 ml min^{-1}
Anions	Dionex™ IonPac™ AS12A 4x50 mm	Dionex™ IonPac™ AS12A 4x200mm	Dionex™ AERS™ 500	2.7mM Na_2CO_3 0.3mM $NaHCO_3$	1 ml min^{-1}

Table S6: List of sample preparations and aliquots for the specific soil solution analyses performed during the incubation.

Analyses	Filter size	Sample volume (ml)	Treatment
Rinse	10 µm	2	-
pH and Eh, Hg/$HgCl_2$	10 µm	4	-
Trace metals	0.02 µm	2	8 ml HNO_3 1%
Trace metals	10 µm	2	8 ml HNO_3 1%
Hg	0.02 µm	3	5 ml (HNO_3 1%, HCl 0.5%)
Hg	10 µm	3	5 ml (HNO_3 1%, HCl 0.5%)
Dissolved organic carbon	0.02 µm	3	5 ml MilliQ + 50 uL 10% HCl
Particulate organic carbon	10 µm	3	5 ml MilliQ + 50 uL 10% HCl
Ion chromatography	0.02 µm	1.5	4.5 ml MilliQ
On days 2, 5, 9 after each flooding.			
AF4	0.45 µm	5	Glovebox under N_2 atmosphere.
Trace metals and Hg	0.45 µm	3	5ml (HNO_3 1%, HCl 0.5%)

Figures

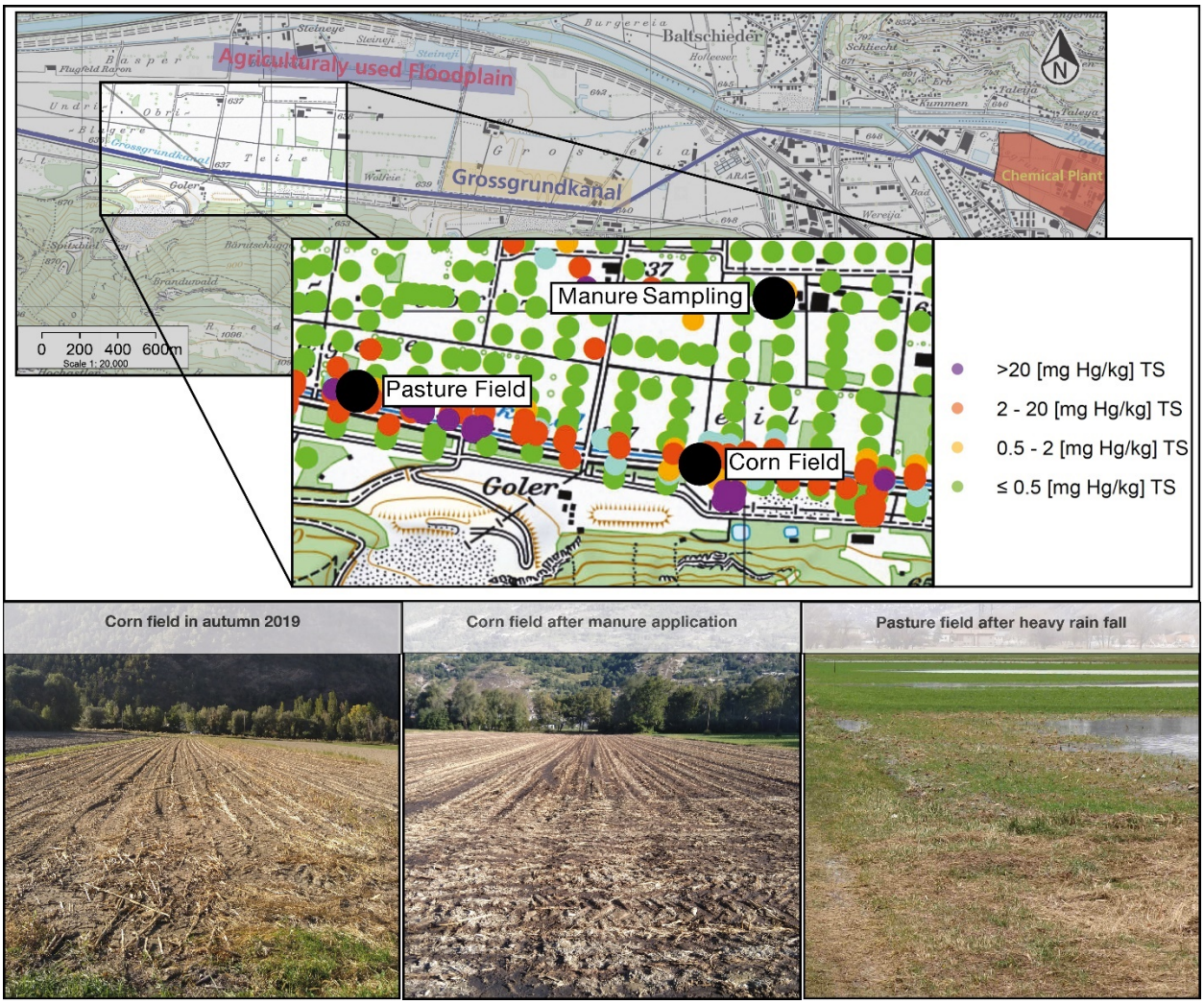

Figure S1: Map and pictures of the sampling location modified after the regional environmental office ("Dienststelle für Umweltschutz") and after (Bundesamt für Landestopografie swisstopo - geo.admin.ch).

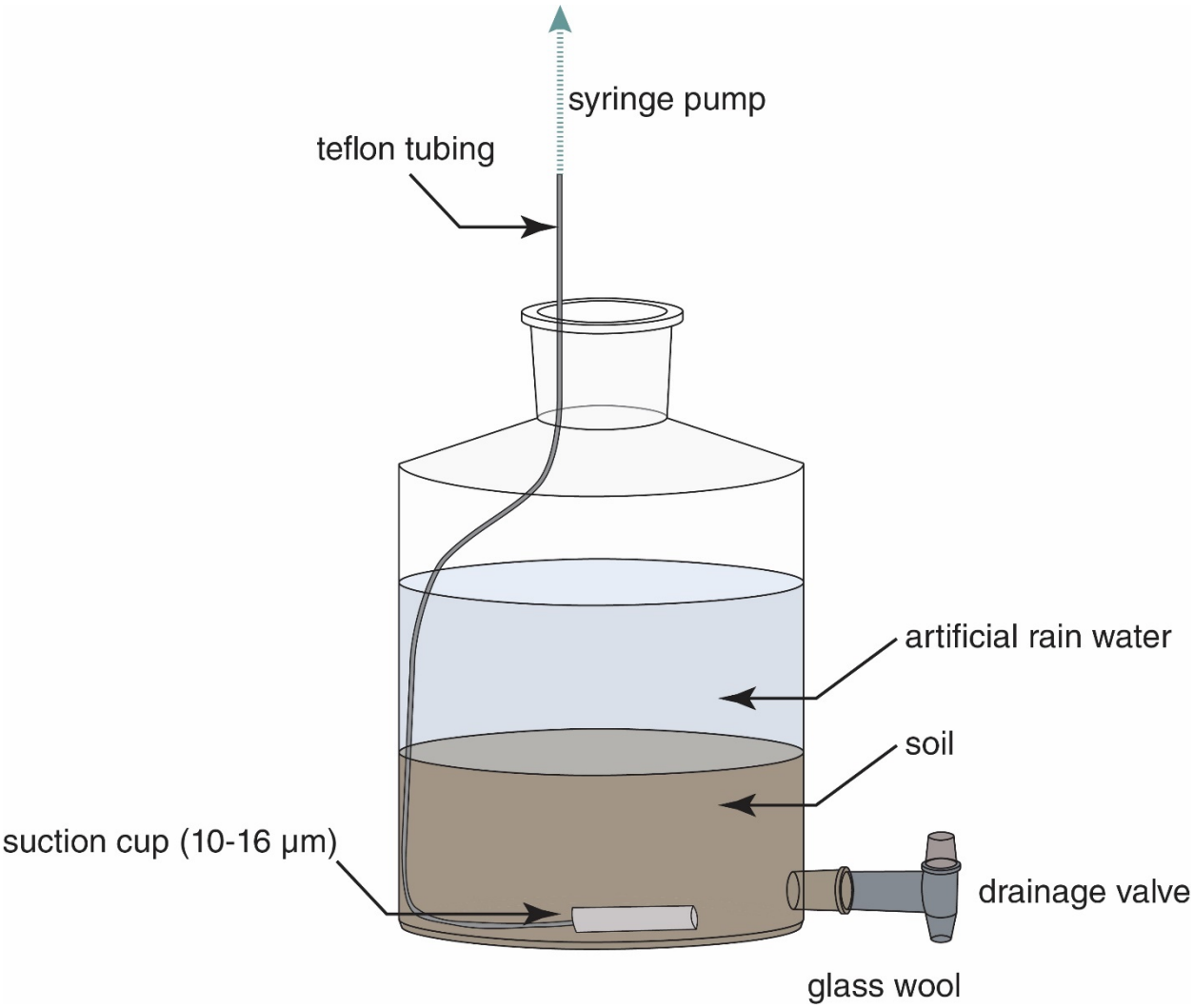

Figure S2: Scheme of the incubation setup. During the incubation the system was covered with parafilm.

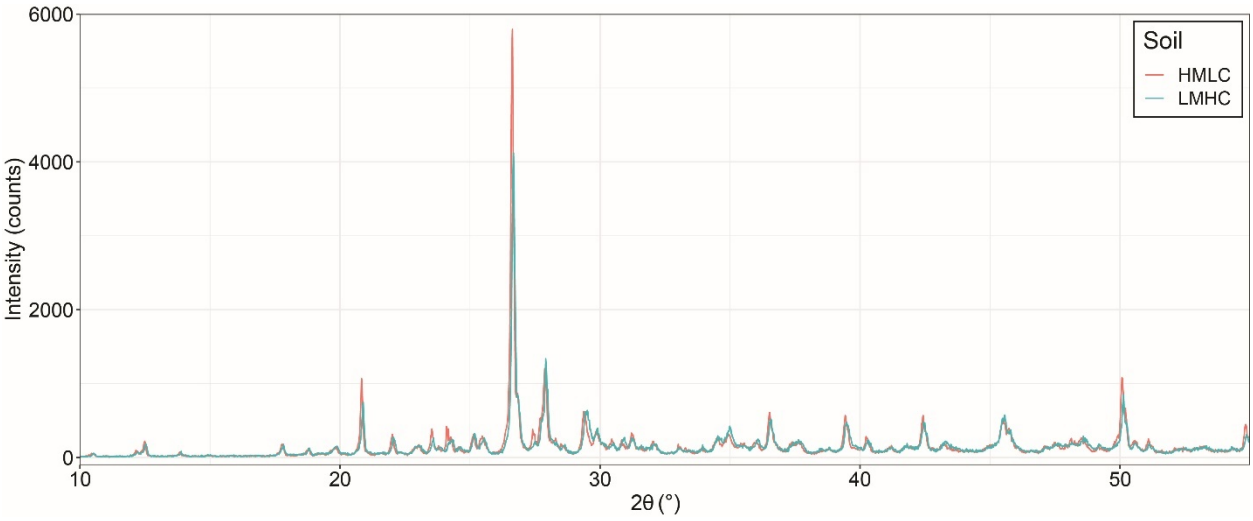

Figure S3: XRD diffractograms of both soil samples used for the incubation (HMLC, LMHC). The overlapping spectra suggest the common origin of parental material of the two soils.

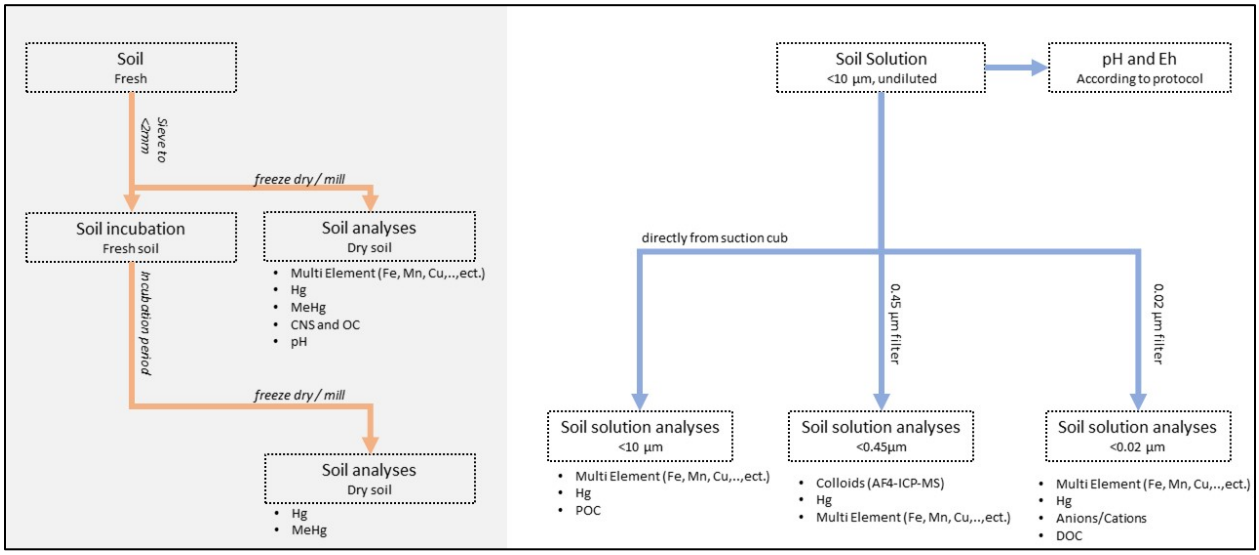

Figure S4: Flow chart of sampling procedure and analyses of soils and soil solution samples.

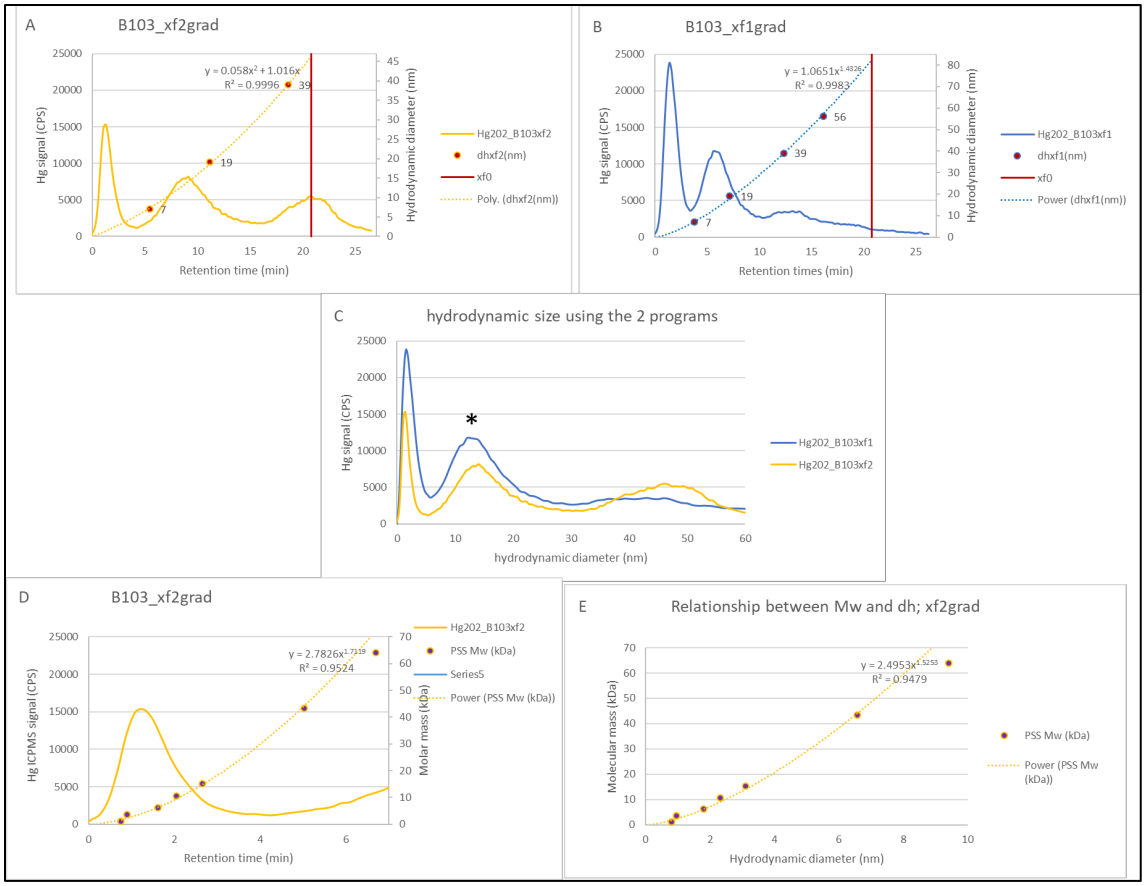

Figure S5: Hydrodynamic size (a, b, c) and small colloids molecular mass (d) calibrations of the elution. The relationship between molecular mass and hydrodynamic diameter is also given in e. Hydrodynamic diameter calibration was obtained using Hc3 (d_h = 7 nm) and ultra-uniform gold nanoparticles (d_h = 19 ; 39 ; 59 nm).

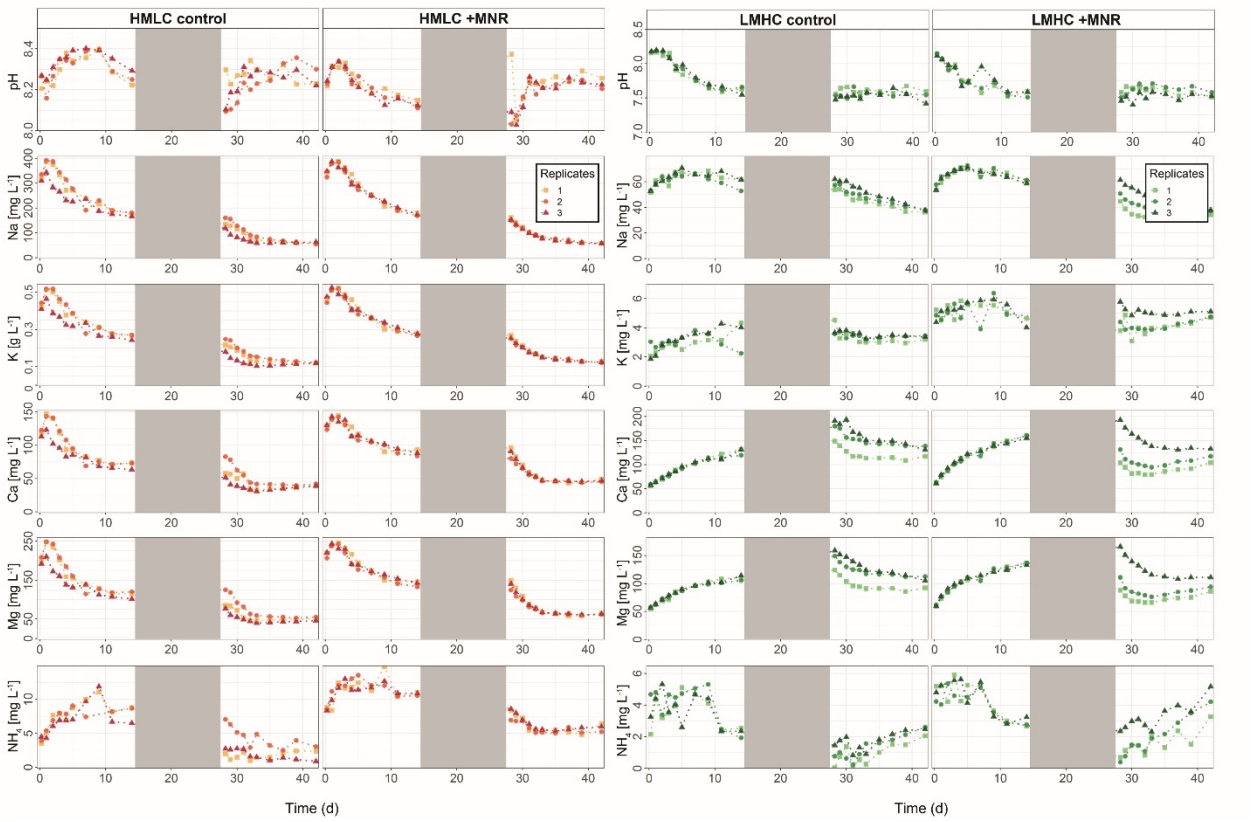

Figure S6: Soil solution time series for pH and major cation concentration of both cornfield (HMLC) in orange and pasture field (LMHC) in green. The gray areas mark the drained period.

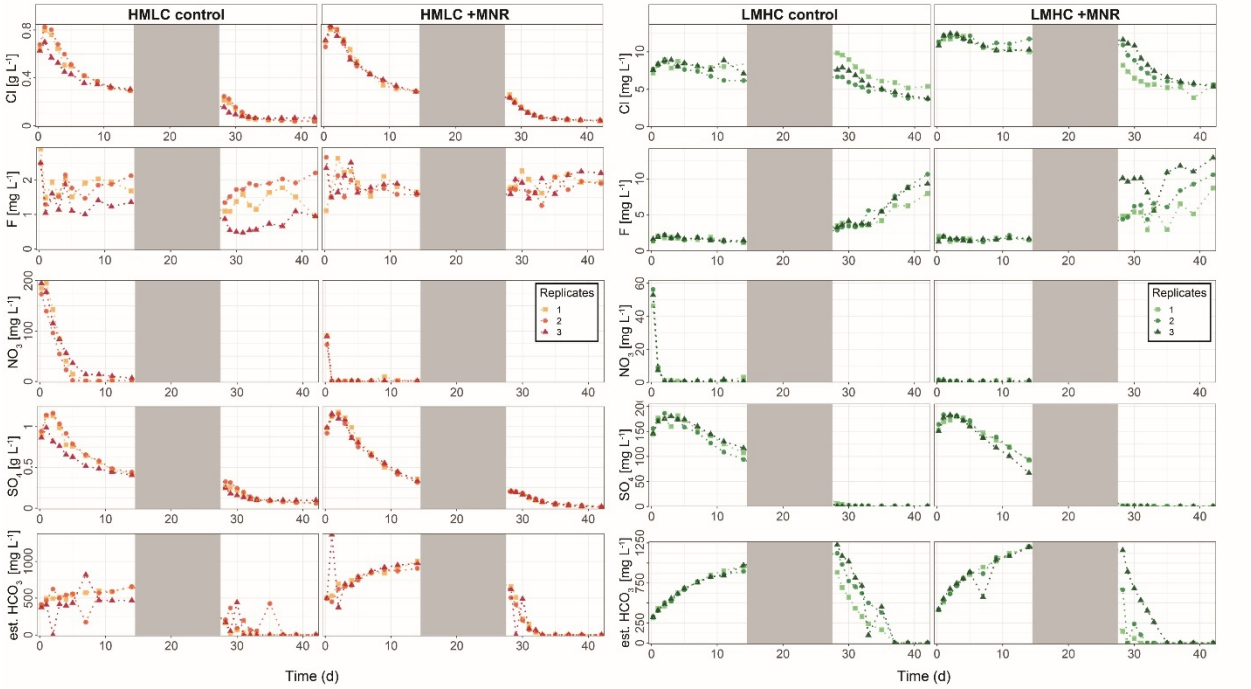

Figure S7: Soil solution time series for major anion concentrations in soil solution of both cornfield (HMLC) in orange and pasture field (LMHC) in green. The gray areas mark the drained period.

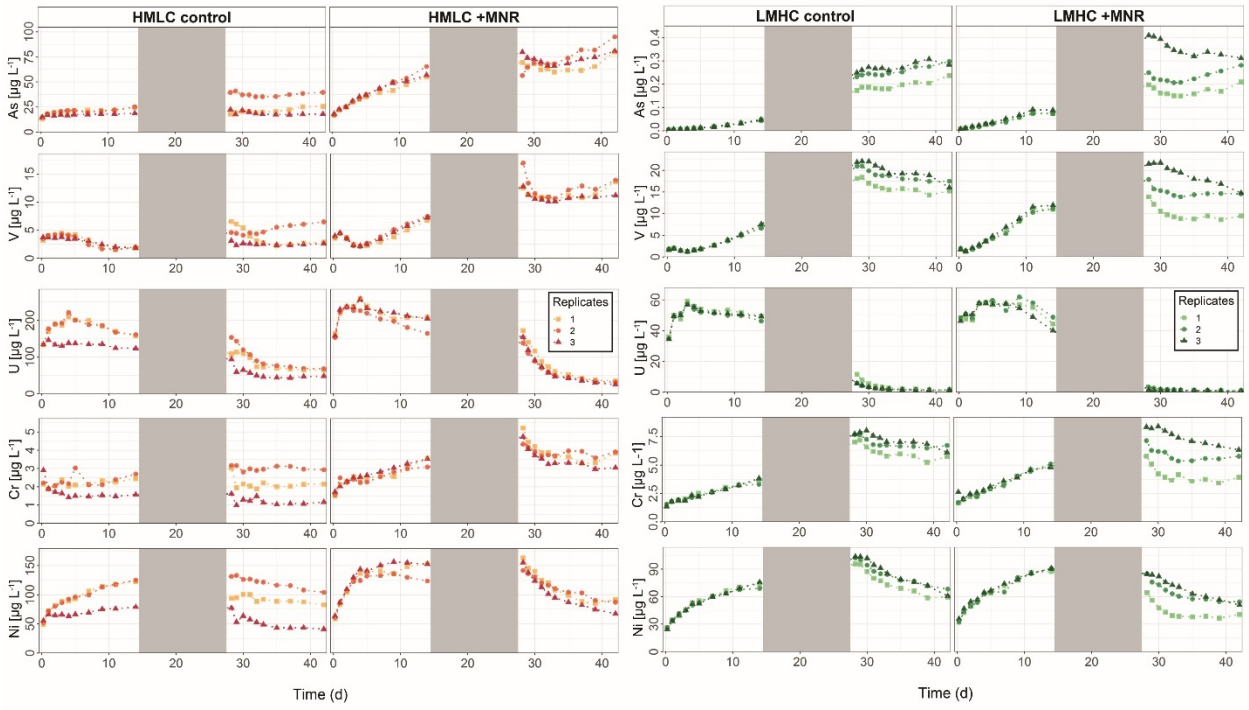

Figure S8: Soil solution time series for redox reactive metal concentrations of both cornfield (HMLC) in orange and pasture field (LMHC) in green. The gray areas mark the drained period.

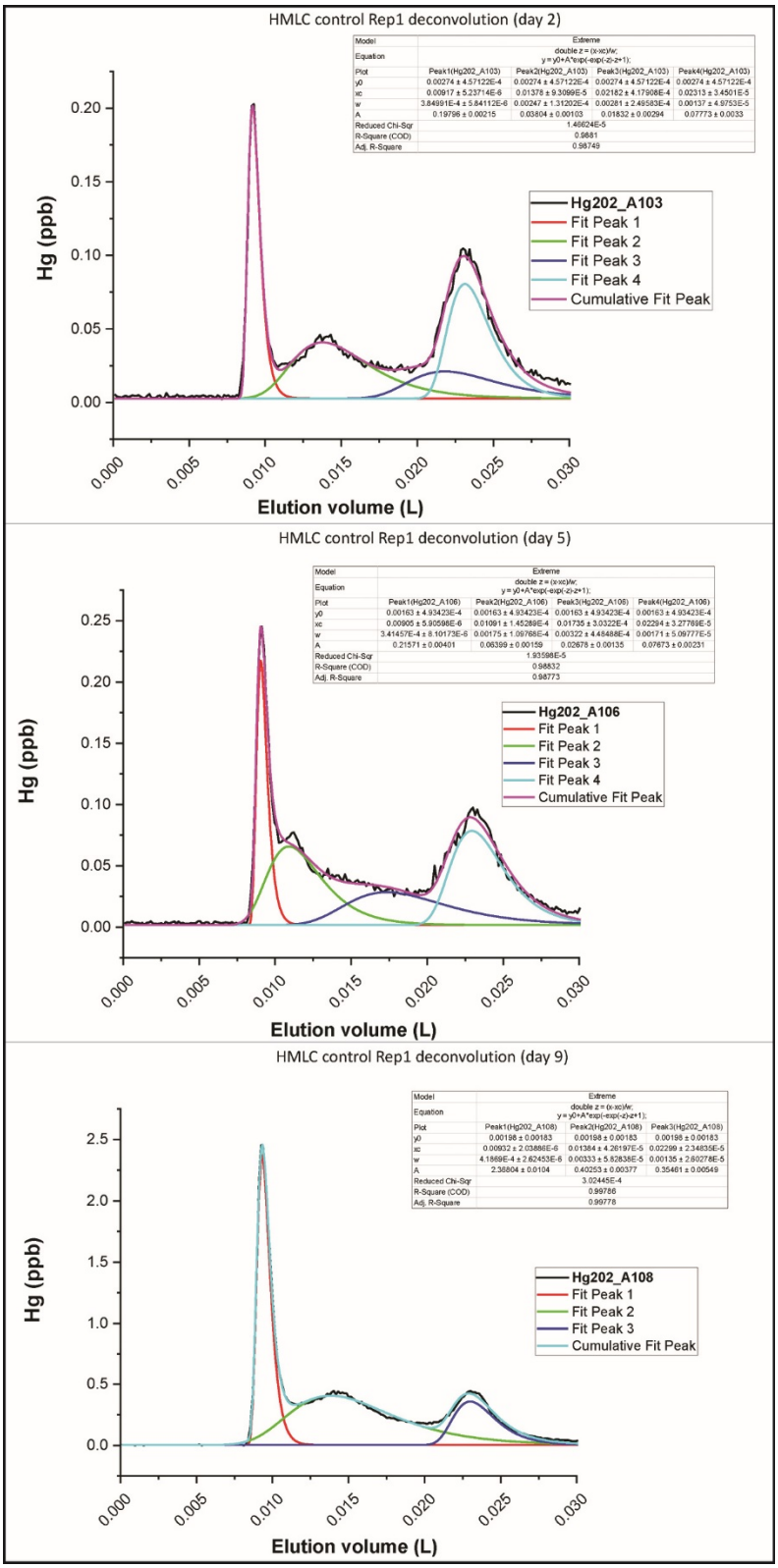

Figure S9: Fractograms and deconvolution for the soil solution samples of HMLC control (Rep1) during the first flooding period.

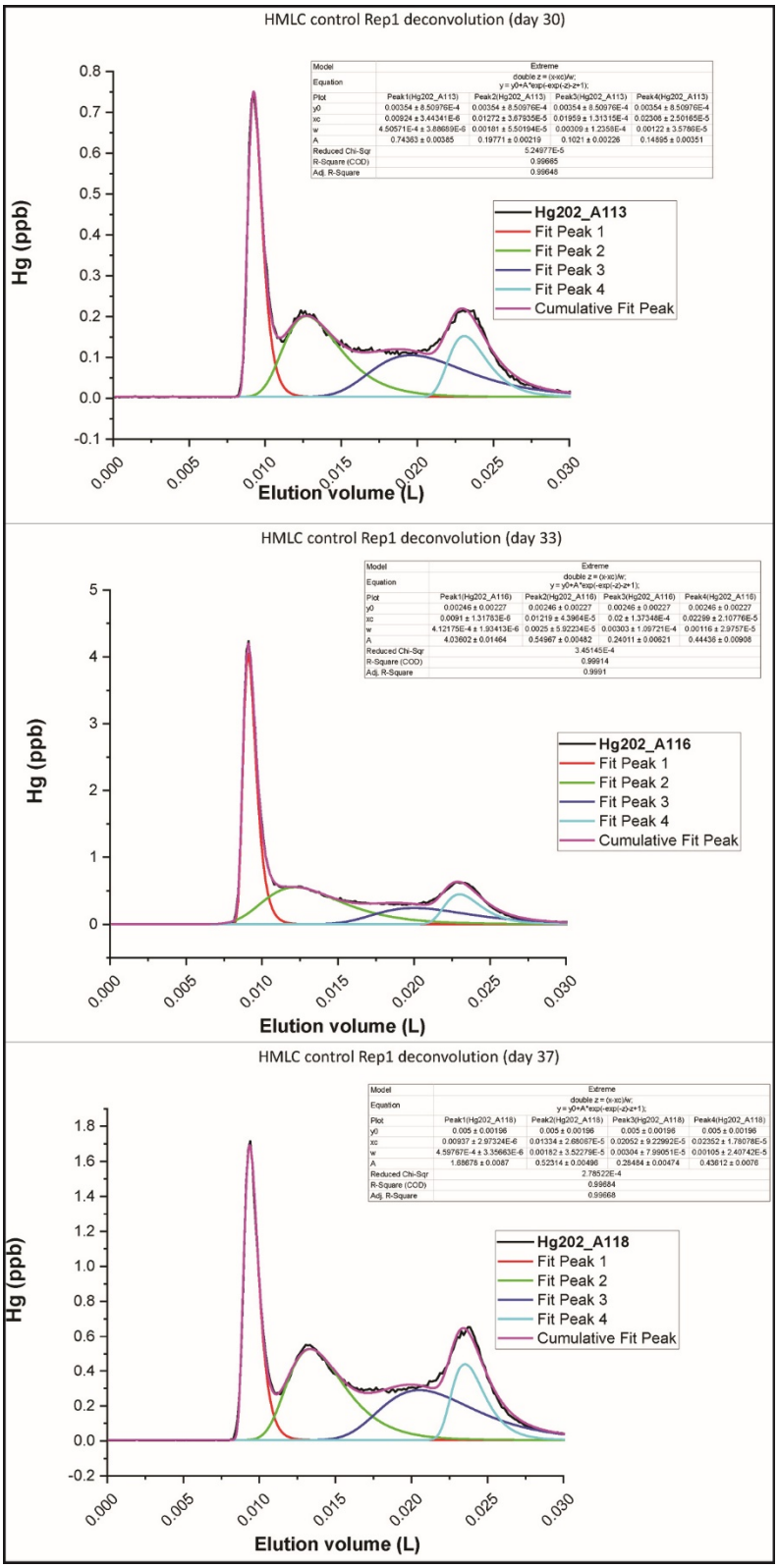

Figure S 10 Fractograms and deconvolution for the soil solution samples of HMLC control (Rep1) during second flooding period.

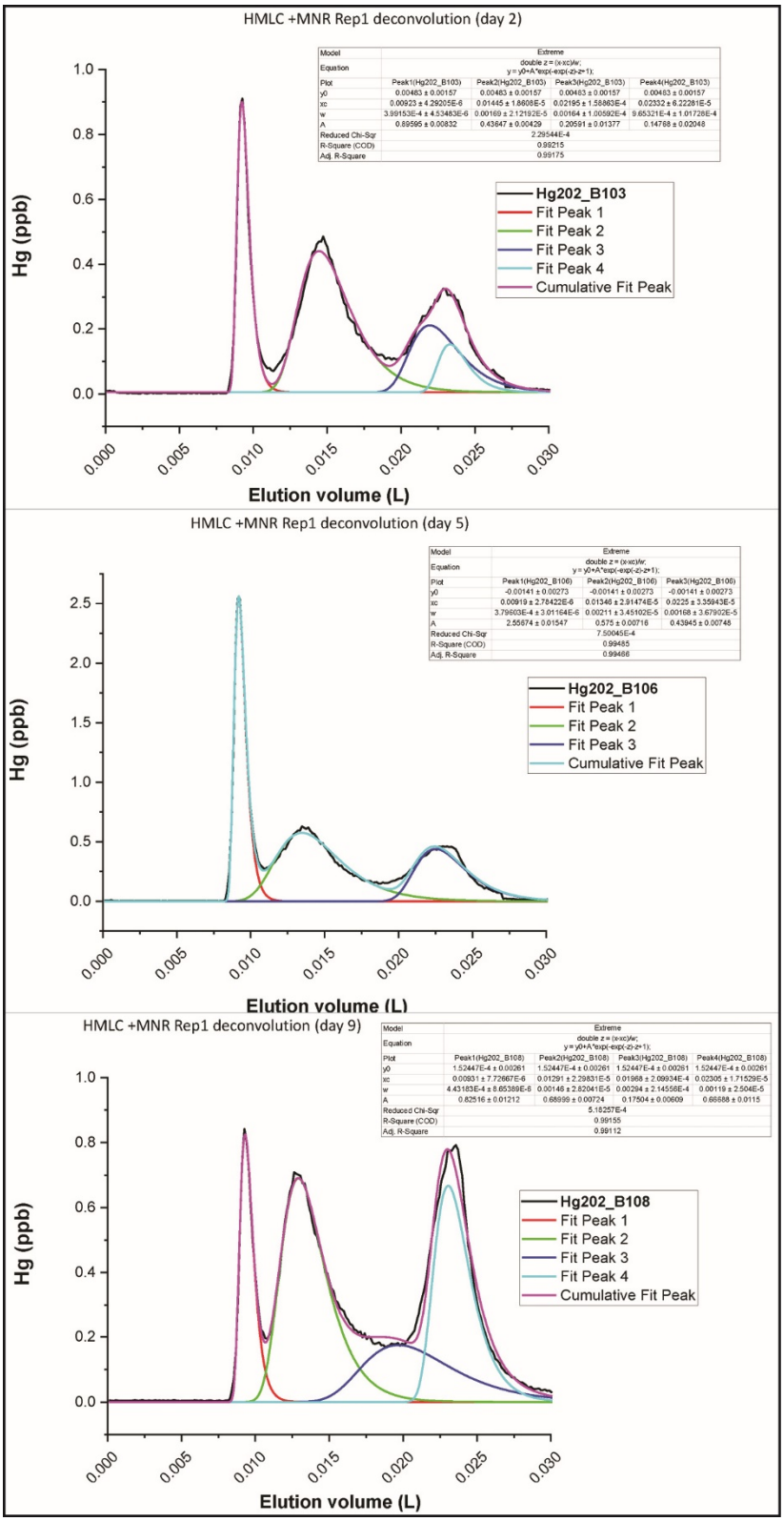

Figure S 11 Fractograms and deconvolution for the soil solution samples of HMLC +MNR (Rep1) during the first flooding period.

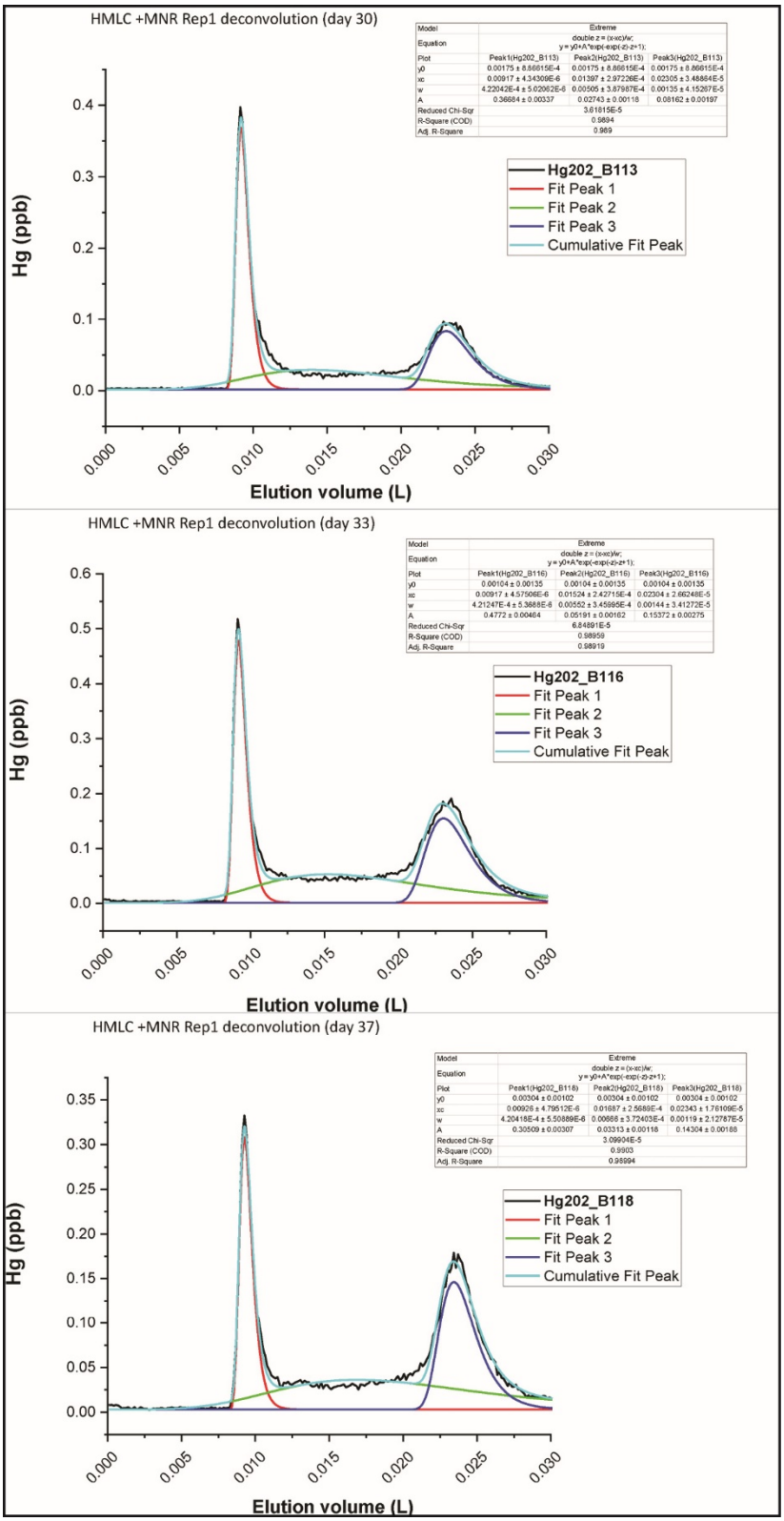

Figure S 12 Fractograms and deconvolution for the soil solution samples of HMLC +MNR (Rep1) during the second flooding period.

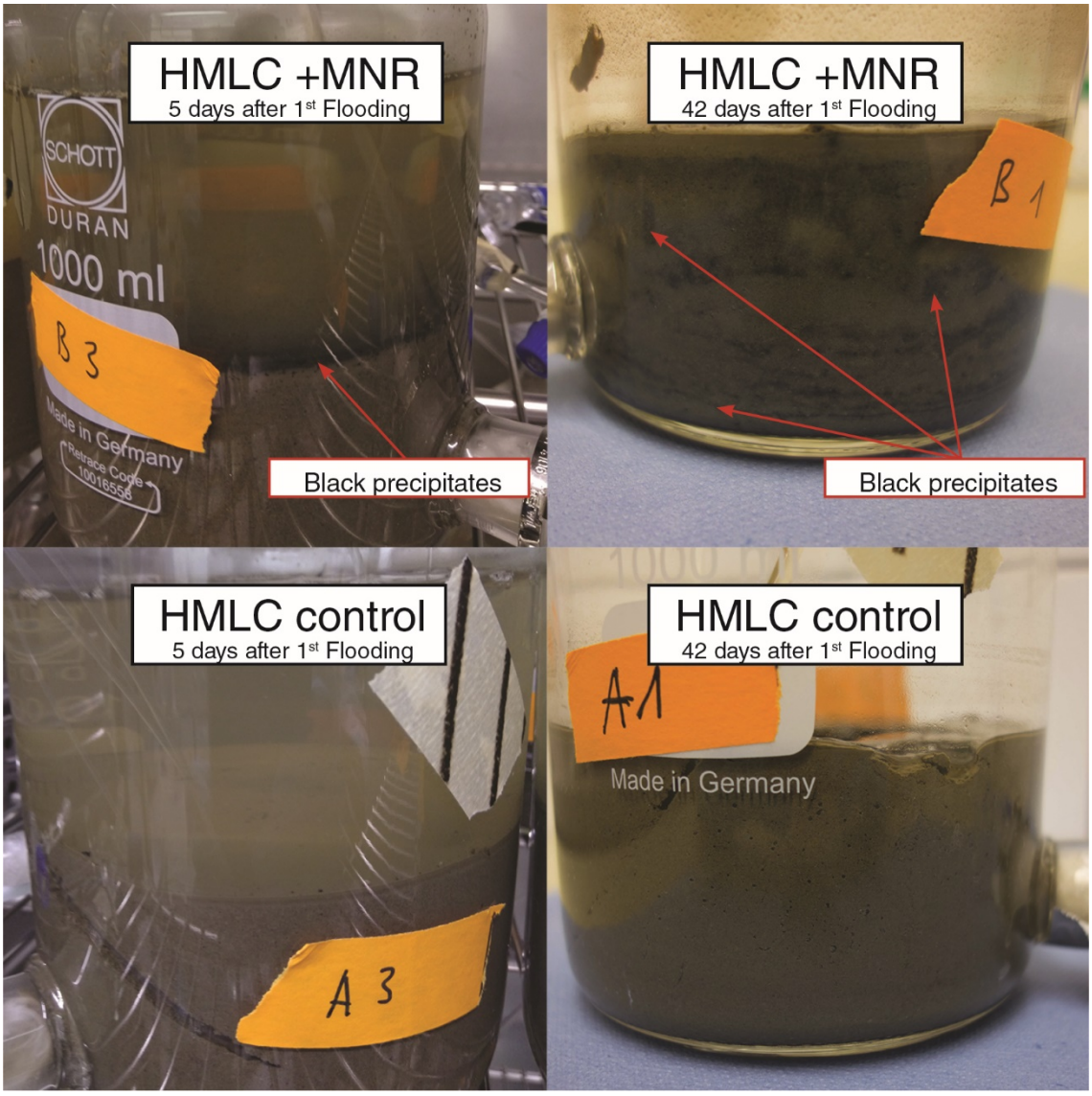

Figure S13: Photographs of MC (HMLC control and HMLC +MNR) after 5 days (left) and 42 days (right) of incubation. In the MCs treated with MNR black precipitates become visible already after 5 days on the top of the soil column and are present in the whole soil column at the end of the incubation experiment.

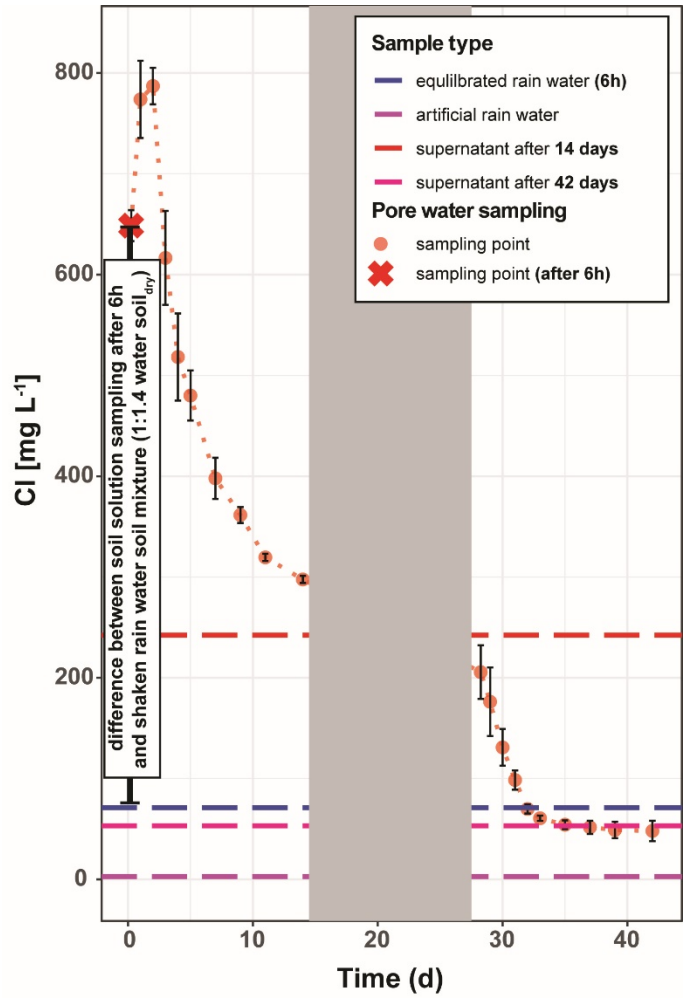

Figure S14: Soil solution chloride concentrations time series of microcosm "HMLC control" (orange), the supernatants at the end of the flooding period (red: 14 days, pink: 42 days), artificial rain water (purple) and equilibrated (6h) rainwater-soil mixture (blue). Gray bar indicates the drained phase during the main incubation. Difference between the sampled soil solution and the equilibrated rainwater-soil mixture are >500 mg L-1 suggesting that solid and liquid phase were not equilibrated with respect to highly soluble minerals at the onset of the incubation.

References

Abgottspon, F., Bigalke, M., and Wilcke, W.: Fast colloidal and dissolved release of trace elements in a carbonatic soil after experimental flooding, Geoderma, 259-260, 156–163, doi:10.1016/j.geoderma.2015.06.005, 2015.

Brombach, C.-C., Gajdosechova, Z., Chen, B., Brownlow, A., Corns, W. T., Feldmann, J., and Krupp, E. M.: Direct online HPLC-CV-AFS method for traces of methylmercury without derivatisation: a matrix-independent method for urine, sediment and biological tissue samples, Analytical and bioanalytical chemistry, 407, 973–981, doi:10.1007/s00216-014-8254-1, 2015.

Erhardt, T., Jensen, C. M., Borovinskaya, O., and Fischer, H.: Single Particle Characterization and Total Elemental Concentration Measurements in Polar Ice Using Continuous Flow Analysis-Inductively Coupled Plasma Time-of-Flight Mass Spectrometry, Environmental science & technology, 53, 13275–13283, doi:10.1021/acs.est.9b03886, 2019.

Frohne, T., Rinklebe, J., Diaz-Bone, R. A., and Du Laing, G.: Controlled variation of redox conditions in a floodplain soil: Impact on metal mobilization and biomethylation of arsenic and antimony, Geoderma, 160, 414–424, doi:10.1016/j.geoderma.2010.10.012, 2011.

Gilli, R., Karlen, C., Weber, M., Rüegg, J., Barmettler, K., Biester, H., Boivin, P., and Kretzschmar, R.: Speciation and Mobility of Mercury in Soils Contaminated by Legacy Emissions from a Chemical Factory in the Rhône Valley in Canton of Valais, Switzerland, Soil Syst., 2, 44, doi:10.3390/soilsystems2030044, 2018.

Glenz, C. and Escher, J.-R.: Voruntersuchung von belasteten Standorten: Histoische Untersuchung Objekt Grossgrundkanal, FUAG-Forum Umwelt AG, Visp, Switzerland, 89 pp., 2011.

Gygax, S., Gfeller, L., Wilcke, W., and Mestrot, A.: Emerging investigator series: mercury mobility and methylmercury formation in a contaminated agricultural flood plain: influence of flooding and manure addition, Environmental science. Processes & impacts, 21, 2008–2019, doi:10.1039/c9em00257j, 2019.

Hojdová, M., Rohovec, J., Chrastný, V., Penížek, V., and Navrátil, T.: The influence of sample drying procedures on mercury concentrations analyzed in soils, Bulletin of environmental contamination and toxicology, 94, 570–576, doi:10.1007/s00128-015-1521-9, 2015.

Li, H., Zheng, D., Zhang, X., Niu, Z., Ma, H., Zhang, S., and Wu, C.: Total and Methylmercury of Suaeda heteroptera Wetland Soil Response to a Salinity Gradient Under Wetting and Drying Conditions, Bulletin of environmental contamination and toxicology, 104, 778–785, doi:10.1007/s00128-020-02874-1, 2020.

Ponting, J., Kelly, T. J., Verhoef, A., Watts, M. J., and Sizmur, T.: The impact of increased flooding occurrence on the mobility of potentially toxic elements in floodplain soil - A review, The Science of the total environment, 754, 142040, doi:10.1016/j.scitotenv.2020.142040, 2020.

Poulin, B. A., Aiken, G. R., Nagy, K. L., Manceau, A., Krabbenhoft, D. P., and Ryan, J. N.: Mercury transformation and release differs with depth and time in a contaminated riparian soil during simulated flooding, Geochimica et Cosmochimica Acta, 176, 118–138, doi:10.1016/j.gca.2015.12.024, 2016.

Weber, F.-A., Voegelin, A., and Kretzschmar, R.: Multi-metal contaminant dynamics in temporarily flooded soil under sulfate limitation, Geochimica et Cosmochimica Acta, 73, 5513–5527, doi:10.1016/j.gca.2009.06.011, 2009.